doi:10.1093/brain/awt204 Brain 2013: 136; 3347–3361 | 3347

BRAIN
A JOURNAL OF NEUROLOGY

Undirected compensatory plasticity contributes to neuronal dysfunction after severe spinal cord injury

Janine Beauparlant,[1,2,*] Rubia van den Brand,[1,2,*] Quentin Barraud,[1,2] Lucia Friedli,[1,2] Pavel Musienko,[1,2,3] Volker Dietz[4] and Grégoire Courtine[1,2]

1 Neurology Department, University of Zurich, Zurich, Switzerland
2 Centre for Neuroprosthetics and Brain Mind Institute, Swiss Federal Institute of Technology (EPFL), Lausanne, Switzerland
3 Russian Academy of Sciences, Pavlov Institute of Physiology, St Petersburg, Russia
4 Spinal Cord Injury Centre, University Hospital Balgrist, Zurich, Switzerland

*These authors contributed equally to this work.

Correspondence to: Grégoire Courtine, PhD.
International Paraplegic Foundation Chair in Spinal cord Repair,
EPFL SV UPCOURTINE - station 19,
1015 Lausanne, Switzerland
E-mail: gregoire.courtine@epfl.ch

Severe spinal cord injury in humans leads to a progressive neuronal dysfunction in the chronic stage of the injury. This dysfunction is characterized by premature exhaustion of muscle activity during assisted locomotion, which is associated with the emergence of abnormal reflex responses. Here, we hypothesize that undirected compensatory plasticity within neural systems caudal to a severe spinal cord injury contributes to the development of neuronal dysfunction in the chronic stage of the injury. We evaluated alterations in functional, electrophysiological and neuromorphological properties of lumbosacral circuitries in adult rats with a staggered thoracic hemisection injury. In the chronic stage of the injury, rats exhibited significant neuronal dysfunction, which was characterized by co-activation of antagonistic muscles, exhaustion of locomotor muscle activity, and deterioration of electrochemically-enabled gait patterns. As observed in humans, neuronal dysfunction was associated with the emergence of abnormal, long-latency reflex responses in leg muscles. Analyses of circuit, fibre and synapse density in segments caudal to the spinal cord injury revealed an extensive, lamina-specific remodelling of neuronal networks in response to the interruption of supraspinal input. These plastic changes restored a near-normal level of synaptic input within denervated spinal segments in the chronic stage of injury. Syndromic analysis uncovered significant correlations between the development of neuronal dysfunction, emergence of abnormal reflexes, and anatomical remodelling of lumbosacral circuitries. Together, these results suggest that spinal neurons deprived of supraspinal input strive to re-establish their synaptic environment. However, this undirected compensatory plasticity forms aberrant neuronal circuits, which may engage inappropriate combinations of sensorimotor networks during gait execution.

Keywords: spinal cord injury; neuronal dysfunction; exhaustion of locomotor activity; compensatory plasticity; syndromic analysis
Abbreviation: SCI = spinal cord injury

Introduction

More than half of human spinal cord injuries lead to permanent paralysis below the level of the injury, as well as severe bladder, bowel, sexual and immune dysfunction (Fawcett *et al.*, 2007; Riegger *et al.*, 2009). There is overwhelming evidence that the dramatic consequences of a severe SCI expand beyond these apparent deficits (Hiersemenzel *et al.*, 2000; Dietz and Muller, 2004; Calancie *et al.*, 2005; Courtine *et al.*, 2009; Dietz *et al.*, 2009; Boulenguez *et al.*, 2010; Murray *et al.*, 2010; Horst *et al.*, 2012). Various

Received February 5, 2013. Revised May 14, 2013. Accepted May 31, 2013. Advance Access publication September 29, 2013

electrophysiological studies have suggested that neuronal circuits deprived of supraspinal input undergo a progressive and extensive remodelling (Calancie *et al.*, 1996, 2000; Maegele *et al.*, 2002; Beres-Jones *et al.*, 2003; Calancie *et al.*, 2005; Harkema, 2008); a process that continues to evolve for years after the SCI (Dietz, 2010). These alterations have been associated with the development of neuronal dysfunction in chronically paralysed individuals. This clinical syndrome is characterized by premature exhaustion of the overall motor neuronal output and poorly coordinated muscle activation patterns during assisted stepping on a treadmill (Dietz and Muller, 2004; Dietz *et al.*, 2009).

Restoration of motor function after severe SCI has been interpreted as the need to regenerate severed fibres to their original target (Tuszynski and Steward, 2012). However, the progressive neuronal dysfunction observed in paralysed individuals emphasizes that recovery of useful sensorimotor capacities after severe SCI will rely on the ability to design interventions that will additionally preserve the integrity of neuronal networks caudal to the injury (Dietz, 2010; Roy and Edgerton, 2012).

A deeper understanding of the mechanisms leading to neuronal dysfunction after severe SCI may contribute to conceptualizing therapeutic strategies capable of counteracting the development of neuronal dysfunction. Various studies in experimental animals uncovered a mosaic of injury-induced molecular and cellular changes in segments caudal to a SCI (Krenz and Weaver, 1998; Ballermann and Fouad, 2006; Kitzman, 2006, 2007; Soares *et al.*, 2007; Hou *et al.*, 2008; Tan *et al.*, 2008; Hou *et al.*, 2009; Boulenguez *et al.*, 2010; Murray *et al.*, 2010; Ichiyama *et al.*, 2011; Singh *et al.*, 2011; Kapitza *et al.*, 2012; Tan *et al.*, 2012). Depending upon the SCI model and specific functional assessments, these alterations in the properties of neuronal circuits have alternatively been classified as beneficial or detrimental. Therefore, the general impending biological principles through which the development of neuronal dysfunction occurs remain unclear.

Although previous studies reported contrasting and variable conclusions, they consistently highlighted the progressive upregulation of receptor (Murray *et al.*, 2010), synapse (Kitzman, 2006; Ichiyama *et al.*, 2011; Kapitza *et al.*, 2012; Tan *et al.*, 2012), and fibre density (Krenz and Weaver, 1998; Ballermann and Fouad, 2006; Hou *et al.*, 2008, 2009) in response to the interruption of supraspinal input. Likewise, ablation of afferent pathways in the brain provokes the formation of new fibre arborizations and spines in the affected region (Kirov and Harris, 1999). This compensatory mechanism has been described as homeostatic plasticity (Turrigiano *et al.*, 1998), a process that strives to maintain the number and strength of synaptic inputs within denervated neuronal circuits. After incomplete SCI that leaves residual motor capacities, activity-dependent mechanisms steer compensatory plasticity in order to restore useful functional capacities (Raineteau and Schwab, 2001; Weidner *et al.*, 2001; Edgerton *et al.*, 2004; Courtine *et al.*, 2008; Rosenzweig *et al.*, 2010). In contrast, more severe SCIs impair the ability to produce movements, which prevents activity-dependent mechanisms from contributing to the remodelling of denervated neuronal networks in a useful direction. The resulting undirected compensatory plasticity may potentially lead to detrimental changes in neuronal circuit properties.

To test this hypothesis, we developed a new rodent model of SCI (Courtine *et al.*, 2008; van den Brand *et al.*, 2012) that replicated the key characteristics of neuronal dysfunction observed in severely paralysed human subjects. Using a range of multifaceted assessments and novel syndromic analysis (Ferguson *et al.*, 2013), we provide evidence suggesting that undirected compensatory plasticity contributes to the development of neuronal dysfunction in the chronic stage of severe SCI.

Materials and methods

Experimental setup

Experiments were conducted on adult female Lewis rats (~220 g body weight). Animals were housed individually on a 12 h light/dark cycle, with access to food and water *ad libitum*. Temperature (22 ± 1°C) and humidity (40–60%) in the animal facilities were maintained constant in accordance to Swiss regulations for animal housing. All animals were handled daily for at least 2 weeks before the first surgeries. Animal care, including manual bladder voiding, was performed twice daily throughout the post-injury period. All procedures and surgeries were approved by the Veterinarian Office of the cantons of Zurich and Vaud, Switzerland.

Surgical procedures and post-surgical care

All surgical procedures used have been described previously (Courtine *et al.*, 2009; Musienko *et al.*, 2011). Under aseptic conditions and general anaesthesia, a partial laminectomy was performed over spinal segments L2 and S1. Stimulating electrodes were created by removing a small part (~1 mm notch) of insulation from Teflon-coated stainless steel wires (AS632, Cooner Wire), which were subsequently secured at the midline overlying spinal level L2 and S1 by suturing the wires to the dura. A common ground wire (~1 cm of Teflon removed at the distal end) was inserted subcutaneously over the right shoulder. Bipolar intramuscular EMG electrodes, using the same wire type, were inserted bilaterally in the medial gastrocnemius and tibialis anterior muscles. All electrode wires were connected to a percutaneous amphenol connector (Omnetics Connector Corporation) fixed to the skull of the rat. Analgesia (buprenorphine Temgesic®, ESSEX Chemie AG, 0.01–0.05 mg per kg, subcutaneous) and antibiotics (Baytril® 2.5%, Bayer Health Care AG, 5–10 mg per kg, subcutaneous) were provided for 5 days post-surgery. After the completion of pre-injury recordings, a second surgery was performed. Partial laminectomies were made at mid-thoracic levels and two lateral hemisections were placed on opposite sides at the T7 (left) and T10 (right) spinal segments. This SCI completely interrupted all direct supraspinal input. The completeness of spinal cord lesions was verified histologically post-mortem.

Kinematic, kinetic and electromyography recordings

The same rats ($n = 11$) participated in kinematic, kinetic and EMG recordings before injury, and 1 week (subacute SCI) as well as 9 weeks (chronic SCI) after injury. Stepping capacities were recorded on a motorized treadmill belt set at a constant speed of 9 cm/s. Animals wore a custom-made jacket especially designed for either bipedal or quadrupedal locomotion (Dominici *et al.*, 2012) that was connected to an automated, servo-controlled body-weight support system (Robomedica Inc). The optimal amount of body weight support

was determined visually. Spontaneous (no facilitation) stepping capacities were recorded for both quadrupedal and bipedal postures, before injury as well as 1 and 9 weeks post-injury. To evaluate the functional capacities of lumbosacral circuits in paralysed rats, we applied an electrochemical neuroprosthesis that transformed lumbosacral circuits from non-functional to highly functional networks (Courtine *et al.*, 2009; Musienko *et al.*, 2011, 2012; van den Brand *et al.*, 2012). Chemical stimulations consisted of a systemic administration of the 5-HT_{2A} receptor agonist quipazine (0.2–0.3 mg per kg, intraperitoneal) and the 5-$HT_{1A,7}$ receptor agonist 8-OHDPAT (0.05–0.3 mg per kg, subcutaneous). The agonists were injected 5 min before behavioural testing. Epidural electrical stimulations (0.2 ms duration, 100–500 μA, 40 Hz) consisted of continuous series of rectangular pulses delivered at 40 Hz over spinal segments L2 and S1 through the chronically implanted electrodes. To evaluate the capacity of lumbosacral circuits to sustain stepping in the chronic stage of SCI, locomotor output was recorded every 7 min in a separate group of rats ($n = 4$) during a bout of continuous stepping (14 min) enabled by electrical epidural stimulation alone. In this condition no chemical stimulations were delivered in order to avoid time-dependent effects of pharmacological agents.

Kinematic, kinetic and electromyography analyses

All procedures used have been detailed previously (Courtine *et al.*, 2009; Musienko *et al.*, 2011; van den Brand *et al.*, 2012). Kinematics of hindlimb stepping were captured by the high speed motion capture system Vicon (Vicon Motion Systems), consisting of 10 infrared cameras (MX-3+, 200 Hz). Reflective markers were attached bilaterally at the iliac crest, the greater trochanter (hip joint), the lateral condyle (knee joint), the lateral malleolus (ankle), the distal end of the fifth metatarsophalangeal joint and the tip of the fourth toe. The body was modelled as an interconnected chain of rigid segments, and joint angles were generated accordingly. Vertical ground reaction forces were recorded using a biomechanical force plate (2 kHz; HE6X6, AMTI) located below the treadmill belt. EMG signals (2 kHz) were amplified, filtered (10–1000 Hz bandpass), stored and analysed offline to compute the amplitude, duration and timing of individual bursts. For both the left and right hindlimbs, 10 successive step cycles were extracted from a continuous sequence of stepping on a treadmill for each rat under each condition. A 10-s interval was used when no or very minimal stepping movements were observed. A total of 147 parameters quantifying gait, kinematics, kinetics and EMG features were computed for each limb and gait cycle according to methods described in detail previously (Courtine *et al.*, 2008, 2009; Musienko *et al.*, 2011; van den Brand *et al.*, 2012).

Electrophysiological experiments

Spinal reflexes were assessed in fully awake rats ($n = 10$). During testing, the animals were suspended in the air (no contact with the ground) using the trunk harness and robotic systems described above. To elicit reflexes, we delivered single rectangular pulses (0.5 ms duration) through the chronically implanted S1 electrode at 0.2 Hz. Before the injury, we identified the stimulus intensity (typically ~160–200 μA) that elicited the largest monosynaptic responses in the absence of direct muscle responses (direct stimulation of the motor nerve, equivalent to M waves), typically 1.5 to 2-fold above motor threshold (Gerasimenko *et al.*, 2006), and used this intensity to test reflexes at 1 and 9 weeks post-injury. The compound motor-evoked potentials were recorded in both left and right tibialis anterior muscles (10 kHz), and the onset latency, peak-to-peak amplitude, and integral of the averaged ($n = 5$) reflex responses were determined.

Tracing procedures

Under general anaesthesia, a laminectomy over L1–L2 spinal level was performed to expose the dorsal aspect of the spinal cord. In a subset of rats with chronic SCI ($n = 6$), a 10% suspension of tetramethylrhodamine-conjugated dextran 3000 MW (TMR) (Invitrogen AG) was stereotaxically injected into the spinal cord, using a 33 G needle on a 10 μl Hamilton syringe (1701 RN, Hamilton Company) attached to an UltraMicroPump (World Precision Instruments). Six injections of 200 nl TMR separated by 700 μm were performed in each hemicord. The injection coordinates were 800 μm lateral of the midline and ~700 μm above the ventral surface of the spinal cord.

To elicit locomotor-related expression of c-fos, the remaining chronic SCI rats ($n = 5$) stepped bipedally on a treadmill during 45 min with the electrochemical neuroprosthesis. Rats were returned to their cages and perfused exactly 60 min after stepping (Ichiyama *et al.*, 2008; Courtine *et al.*, 2009). All animals were deeply anaesthetized by an intraperitoneal injection of 0.5 ml pentobarbital-Na (50 mg/ml) and transcardially perfused with ~80 ml Ringer's solution containing 100 000 IU/l heparin (Liquemin, Roche) and 0.25% $NaNO_2$ followed by 300 ml of cold 4% phosphate buffered paraformaldehyde, pH 7.4 containing 5% sucrose. The brain and spinal cord were removed and postfixed overnight in the same fixative before they were transferred to 30% sucrose in phosphate buffer for cryoprotection. The tissue was embedded in Tissue Tek O.C.T (Sakura Finetek Europe), frozen at −40°C, and cut to a thickness of 30 or 40 μm.

Immunohistochemistry

Mounted or free-floating sections were washed three times in 0.1 M PBS and blocked in 5% normal goat serum containing 0.3% Triton. For c-fos and neurofilament stainings, slices were pretreated with H_2O_2 and cold methanol (100%), respectively. Sections were then incubated in primary antibody diluted in the blocking solution overnight at 4°C (c-fos) or room temperature (neurofilament, vGlut1, vGlut2). TMR visualization incubation time was 48 h at 4°C. The primary antibodies used were rabbit anti-c-fos (1:5000; Santa Cruz Biotechnologies) and anti-TMR (1:1000; Molecular Probes, Life Technologies), mouse anti-neurofilament (1:10 000; Millipore) and anti-vGlut2 (1:5000; Millipore), and guinea pig anti-vGlut1 (1:2000; Millipore) antibodies. Sections were again washed three times in 0.1 M PBS and incubated with the appropriate secondary antibody diluted 1:200 (Alexa fluor® 488 or Alexa fluor® 555; Molecular Probes, Life Technologies) in blocking solution. Sections were washed again, mounted onto glass slides, and coverslipped with Mowiol®.

Neuromorphological evaluations

TMR-labelled fibres and c-fos-positive neurons were counted using image analysis software (Neurolucida, MicroBrightField) on 4–5 transverse slices per animal. For TMR-labelled fibres, a rectangular grid half the size of the ventral horn was overlaid and intersecting fibres within the grey matter were counted. C-fos-positive neurons were quantified with respect to the Rexed laminae defined by Molander *et al.* (1984). Neurofilament and vesicular glutamate transporter (vGlut1, vGlut2) density was measured using three to five confocal image stacks per region per rat acquired with standard imaging settings and analysed using custom-written Matlab (MathWorks) scripts according to previously described methods (Carmel *et al.*, 2010; van den Brand *et al.*,

2012). Confocal output images were divided into square regions of interest, and densities computed within each region of interest as the ratio of traced fibres (amount of pixels) per region of interest area. Both manual and computerized counts were performed blindly. Image acquisition was performed using a Leica TCS SPE or SP5 laser confocal scanning microscope and the LAS AF interface (Leica Microsystems) and stacks were processed offline using the Imaris software (Bitplane).

Principal component analysis

To evaluate the characteristics underlying stepping for the different experimental conditions, we implemented a multi-step statistical procedure based on principal component analysis (Courtine *et al.*, 2009; Musienko *et al.*, 2011; Dominici *et al.*, 2012). The various steps, methods, typical results, and interpretation of the analysis are detailed in Figs 2 and 3. The same procedure was applied for the syndromic analysis; all the collected kinematic, kinetic, EMG, electrophysiological, neuromorphological and immunohistochemical parameters of SCI animals ($n = 6$) were manually curated and combined in a single matrix.

Comparisons with neuronal dysfunction in humans with severe injury

Electrophysiological recordings of leg muscle activity and spinal reflex behaviour were conducted in individuals with motor complete (Dietz *et al.*, 2009; Hubli *et al.*, 2012) or motor incomplete SCI (Hubli *et al.*, 2012). To evaluate the capacity of spinal neuronal networks to sustain locomotion, we recorded the EMG activity of the tibialis anterior and medial gastrocnemius muscles during 10–15 min of robotically assisted stepping at a constant speed of 2.0 km/h and 65–75% body weight support. Spinal reflex behaviour was assessed in healthy subjects, as well as in spinal cord injured individuals in the early and late stage of SCI. Non-noxious electrical stimuli were randomly applied to the distal part of the tibial nerve in subjects wearing a harness in an upright, unloaded position, as performed in the rats. Each stimulation was composed of a series of eight biphasic rectangular stimuli with 2 ms single stimulus duration and a frequency of 200 Hz. Stimulation intensity was set at two times motor threshold. Reflex responses were recorded from the ipsilateral tibialis anterior muscle.

Statistical procedures

All data are reported as mean values ± SEM. Statistical evaluations were performed using one-way ANOVA for neuromorphological evaluations, and one- or two-way repeated-measures ANOVA for functional assessments. The *post hoc* Tukey's or Fisher LSD test was applied when appropriate. Pearson's correlation coefficients were used to evaluate univariate correlations, except for patient data where the Spearman's rank correlation coefficient was computed. The significance level was set as $|R \text{ value}| > 0.45$ and $P < 0.05$, respectively.

Results

Staggered hemisection injury leads to complete and permanent paralysis

Adult rats received a severe SCI consisting of a left lateral hemisection at T7 and right lateral hemisection at T10, which interrupted all the direct supraspinal input to lumbosacral circuits (van den Brand *et al.*, 2012). To test the functional impact of the SCI, we positioned the rats bipedally and quadrupedally on a motorized treadmill (9 cm/s) with robot-assisted vertical support (% of body weight support). In both postures, the rats showed continuous dragging of both hindlimbs along the treadmill belt, which was associated with the absence of EMG activity in flexor and extensor muscles of the ankle (Fig. 1B and C). Occasionally, some of the tested rats exhibited spontaneous hindlimb oscillations, either unilateral or bilateral, which rapidly extinguished after a few cycles, as previously observed in rats with complete SCI (Courtine *et al.*, 2009).

Staggered hemisection injury leads to neuronal dysfunction in the chronic stage

We sought to evaluate the functional properties of lumbosacral locomotor circuits in the subacute (1 week post-injury) and chronic stage (9 weeks post-injury) of the SCI ($n = 9$). To enable locomotion of the paralysed hindlimbs, we applied an electrochemical neuroprosthesis that transformed lumbosacral circuits from non-functional to highly functional networks (Courtine *et al.*, 2009; Musienko *et al.*, 2012). By increasing the general level of spinal excitability, this electrochemical spinal neuroprosthesis enables sensory information to become a source of control for stepping. In consequence, the recorded motor patterns were exclusively generated within lumbosacral circuits, without contribution from supra-lesional input (Courtine *et al.*, 2009; van den Brand *et al.*, 2012). As early as 1 week post-lesion, electrochemical stimulations promoted coordinated locomotion with appropriate timing of left and right limb alternation, and reciprocal activation between flexor and extensor muscles (Fig. 1A and B). In striking contrast, the same rats exhibited highly variable stepping patterns with poor inter- and intra-limb coordination in the chronic stage of the SCI (Fig. 1C).

We next aimed at quantifying gait performance pre-injury, and at the subacute and chronic stages of SCI. To achieve this, we applied a multi-step statistical procedure based on principal component analysis. We first conducted detailed kinematic, kinetic and EMG recordings, which allowed the computation of a large number of variables ($n = 147$) that provided a comprehensive quantification of gait patterns for each rat and time point. Principal component analysis creates new variables that linearly combine the original parameters in order to maximize the amount of explained variance per principal component analysis. Individual gait cycles can be represented in the new de-noised space defined by the first three principal component analyses. Gait patterns associated with each experimental time point emerged in distinct spatial locations (Fig. 2A). To visualize these differences, we applied a least square elliptic fitting on each cluster. The distance between data points in the principal component analysis space provides a measure of the degree of discrepancy or similarity between the clusters, i.e. gait patterns (Fig. 2B). The dispersion of data points accounts for the variability of gait patterns within each rat and time point (Fig. 2B). This analysis revealed that gait patterns recorded in the chronic stage significantly

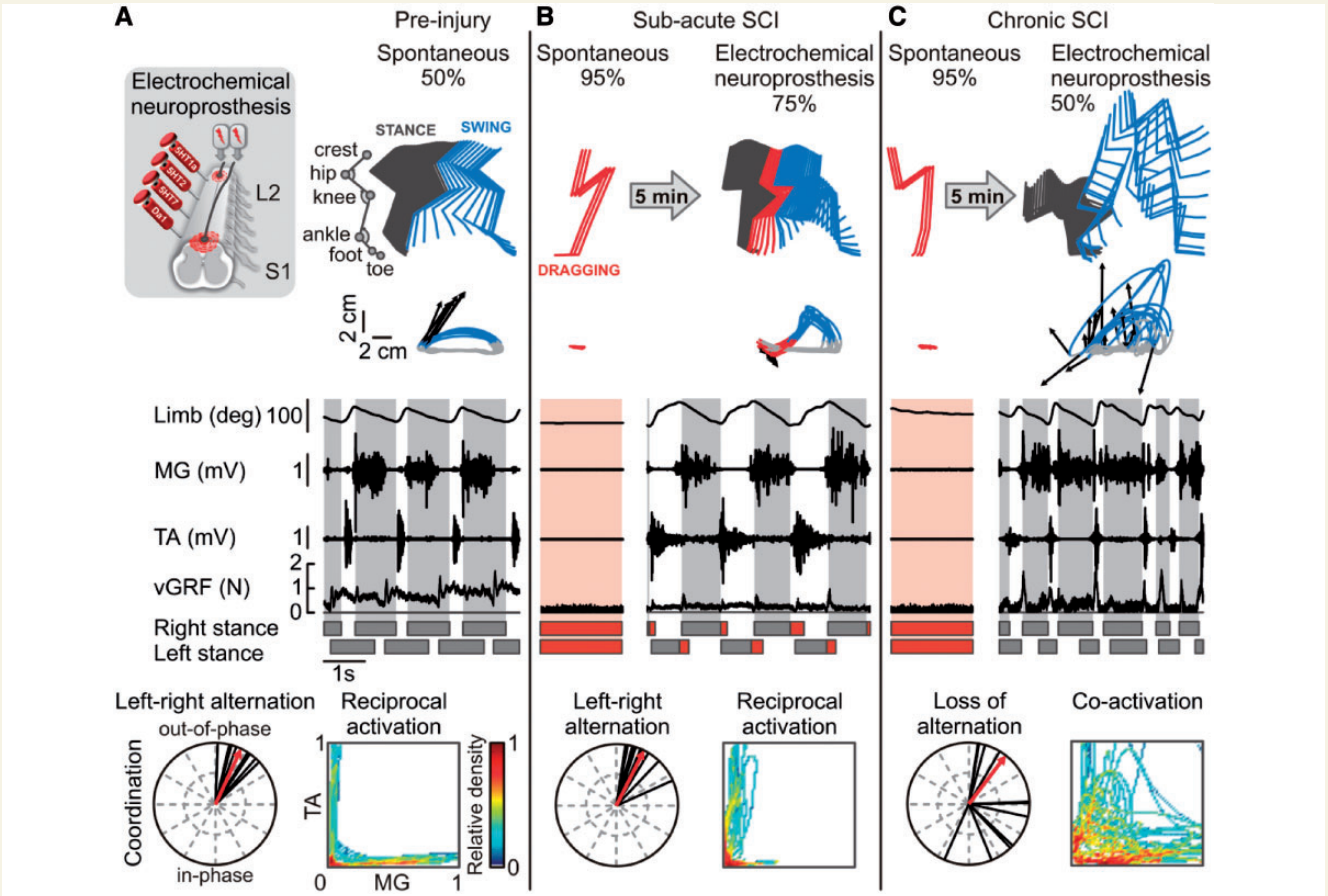

Figure 1 The staggered lateral hemisection SCI led to deterioration of locomotor function in the chronic stage. (**A**) Diagram of the electrochemical neuroprosthesis. Rats were positioned bipedally over a moving treadmill belt and provided with body weight support. A representative locomotor trial of the same rat performed before injury (intact), (**B**) 1 week (subacute SCI) and (**C**) 9 weeks post-injury (chronic SCI) is shown. Above each panel, the % of body weight support is indicated and a stick diagram decomposition of hindlimb motion is shown together with colour-coded trajectories of hindlimb endpoints. Vectors represent the direction and intensity of the hindlimb endpoint velocity at swing onset. The corresponding sequences of hindlimb oscillations, raw EMG activity of an extensor (MG, medial gastrocnemius) and a flexor (TA = tibialis anterior) muscle and vertical ground reaction forces (vGRF) are shown below. Grey and red bars indicate the duration of stance and drag phases, respectively. For each time point, a polar plot representation illustrates the coordination between the oscillations of left and right hindlimbs (black line, single gait cycle; red arrow, average of all gait cycles). The density plot displays the coordination between the antagonistic muscles tibialis anterior and medial gastrocnemius throughout one locomotor trial. L-shaped patterns reflect perfect reciprocal activation of muscles.

differed from ($P < 0.01$), and showed a high gait variability compared with ($P < 0.05$) those observed in the same rats pre-injury and in the subacute stage ($n = 9$). Principal component analysis scores indicate the location of data points and conditions along each individual principal component analysis axis (Fig. 2C). Here, extraction of scores revealed that PC1 captured differences across the time points ($P < 0.001$), whereas PC2 distinguished the subacute stage from the other time points ($P < 0.01$). Next, we computed the factor loadings, which correspond to the correlation between each variable and each principal component analysis. We then identified variables with significant factor loading ($|value| > 0.5$, $P < 0.05$), which we regrouped into functional clusters that we named for clarity (Fig. 3A). To provide a more classical representation of differences between time points, histogram plots were generated for the most prominent variable (highlighted within yellow frames; Fig. 3A) per extracted functional cluster in PC1 (Fig. 3B) and PC2 (Fig. 3C). This multi-step analysis showed that in the chronic stage of the SCI rats exhibited highly variable gait patterns, a pronounced flexed posture, poor interlimb coordination, altered distal joint control, and enhanced extensor muscle activation during electrochemically-enabled locomotion (PC1 clusters; Fig. 3B). Instead, slow movement, low level of weight bearing, and prolonged swing duration characterized gait patterns underlying stepping in the subacute stage (PC2 clusters; Fig. 3C). Together, these results not only emphasize the dramatic degradation of stepping capacities in the chronic stage of SCI, but also identify the ensemble of gait features that characterizes the syndromic signature of this neuronal dysfunction. We sought to leverage this detailed evaluation to decipher putative mechanisms underlying these functional changes.

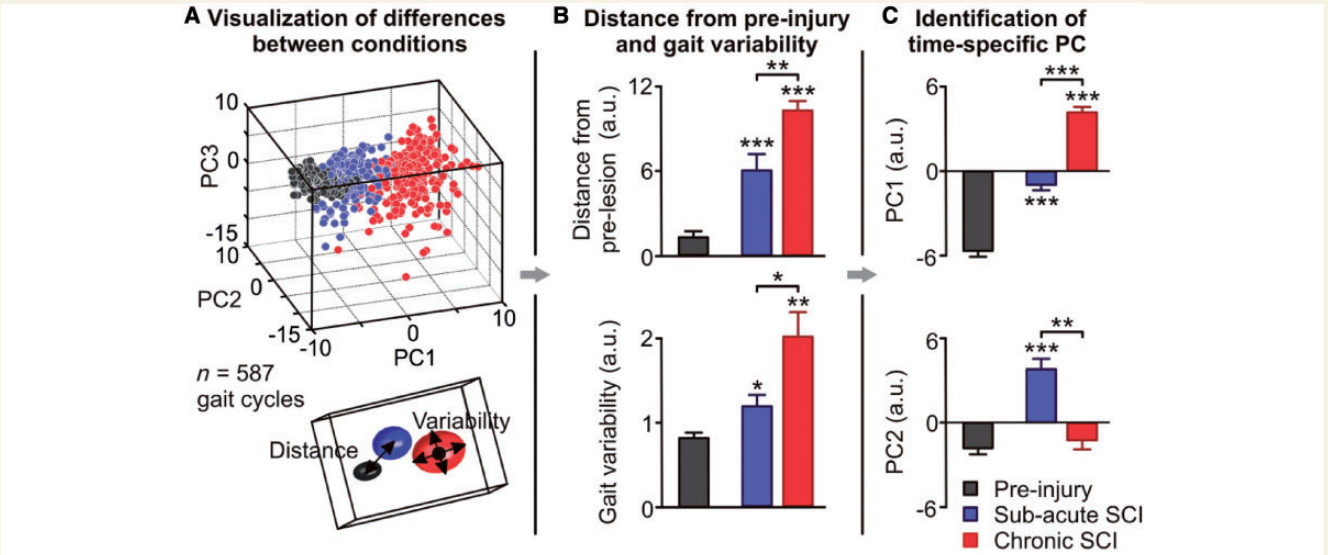

Figure 2 Multi-step statistical analysis of gait patterns. (**A**) Representation of individual gait cycles in the new de-noised space created by PC1–3. Least square elliptic fitting reveals widely separated clusters of data points for each time point. (**B**) Locomotor performances were quantified, for each rat, as the 3D Euclidean distance between the location of gait cycles and the average location of all gait cycles from the same rats pre-lesion ($n = 9$ rats). Variability of gait cycles was assessed as the dispersion of data points for each rat and time point. (**C**) The scores indicate which experimental time points are differentiated by each principal component (PC). $*P < 0.05$; $**P < 0.01$; $***P < 0.001$. Error bars, SEM.

Staggered hemisection injury leads to premature exhaustion of locomotor muscle activity

Chronically injured, non-ambulatory SCI patients showed premature exhaustion of leg muscle activity during robotically assisted locomotion (Fig. 4C; adapted from Dietz *et al.*, 2009). We tested whether rats with a severe, chronic SCI exhibited a similar decrease in hindlimb muscle activation during electrically enabled stepping (Fig. 4A). At the onset of stepping, the electrical neuroprosthesis promoted coordinated locomotor movements with alternation between powerful bursts of EMG activity in flexor and extensor muscles. The recruitment of hindlimb muscles rapidly declined over time, and eventually reached amplitudes that were too low to sustain locomotion ($P < 0.05$; Fig. 4B). Similar exhaustion of locomotor EMG was observed during manually assisted movements in rats (data not shown). These results show that, as observed in humans, rats exhibited premature exhaustion of the overall locomotor muscle output in the chronic stage of a severe SCI.

Staggered hemisection injury leads to the emergence of abnormal long-latency reflex responses

In severely paralysed humans, exhaustion of locomotor muscle activity occurred in parallel with the emergence of abnormal, long-latency reflex responses in leg muscles (Dietz *et al.*, 2009). To elicit these reflexes, a train of stimuli was applied to the tibial nerve in upright and unloaded human subjects. In the absence of neurological impairments, the stimulation evoked a short-latency (75–100 ms) reflex response in the ipsilateral tibialis anterior muscle (Fig. 5A). Reflex responses with similar latency but markedly reduced amplitude were recorded in the subacute stage of the injury (2 months post-SCI). Chronic, non-ambulatory SCI patients showed a diminished or nearly absent, early reflex response, and concurrently developed an abnormal, long-latency reflex response (200–300 ms) (Fig. 5A). The relative amplitude of this long-latency reflex response inversely correlated with locomotor capacities (Fig. 5E).

We investigated whether similar changes in hindlimb reflex responses occurred in severely paralysed rats. Before the SCI, electrical stimulation delivered through the S1 epidural electrode in fully awake rats elicited two well-defined reflex responses in the tibialis anterior muscle (Fig. 5B), which engaged a monosynaptic and a polysynaptic neural circuit (Gerasimenko *et al.*, 2006). As previously described (Lavrov *et al.*, 2006), the polysynaptic response corresponds to the short latency reflex response evoked in humans. In the subacute stage of the SCI, the polysynaptic response was either markedly reduced or completely suppressed (Fig. 5B). The same rats tested in the chronic stage of the SCI displayed a new, long-latency reflex response in the tibialis anterior muscle (25–50 ms, $P < 0.001$; Fig. 5B and C). Although epidural electrical stimulation primarily recruits afferent fibres (Courtine *et al.*, 2009; Musienko *et al.*, 2012), including the tibial nerve, these responses might not be completely equivalent to those observed in humans. As previously described in human patients, however, the amplitude of this abnormal long-latency

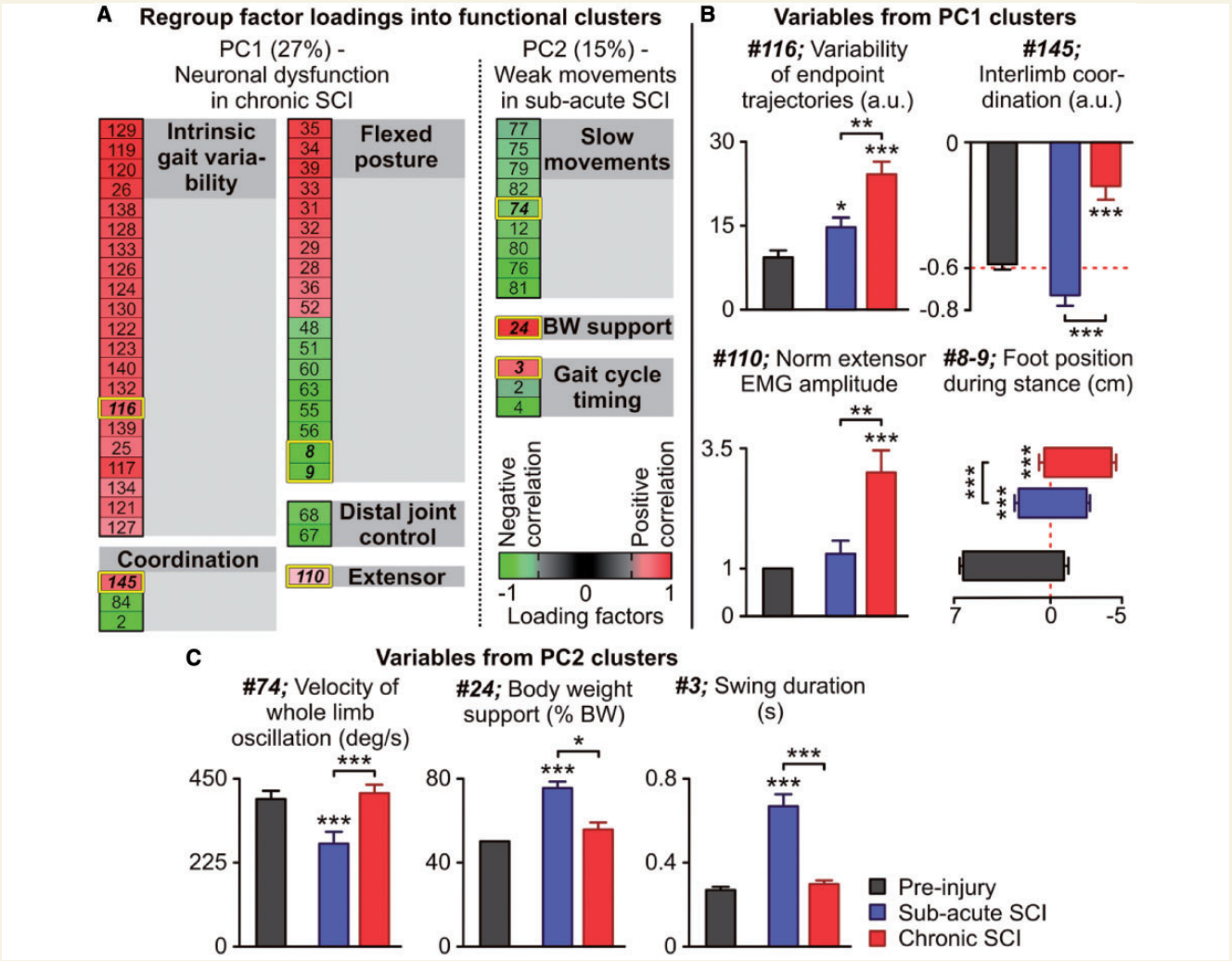

Figure 3 Multi-step statistical analysis identified time-specific features of locomotor patterns after severe SCI. (**A**) Extraction of factor loadings, i.e. correlation between gait variables and the first two principal component analyses. Variables with the highest factor loading (lvaluel > 0.5, $P < 0.05$) were regrouped into functional clusters, which are named for clarity. (**B** and **C**) Bar graphs of single variables [highlighted within yellow frames in (**A**)] for each extracted functional cluster of (**B**) PC1 and (**C**) PC2 ($n = 9$ rats). *$P < 0.05$; **$P < 0.01$; ***$P < 0.001$. Error bars, SEM. BW = body weight.

reflex response inversely correlated with locomotor capacities in rats (r = 0.66, $P < 0.05$; Fig. 5D).

Staggered hemisection injury triggers extensive reorganization within denervated neuronal networks

We surmised that the neuronal dysfunction syndrome, characterized by degradation of stepping capacities, premature EMG exhaustion and abnormal reflex responses, was in part due to abnormal rewiring of the denervated lumbosacral networks. To test this hypothesis, we first assessed putative changes in overall fibre density in spinal segments caudal to the SCI (Fig. 6A). Evaluation of neurofilament staining at spinal segment L4 revealed a 28% decrease in fibre density in intermediate and ventral laminae in the subacute phase compared with intact rats ($P < 0.001$; Fig. 6B). After the complete interruption of supraspinal pathways, severed axons show a rapid Wallerian degeneration (Hausmann, 2003) that likely accounted for this pronounced loss of neurofilament in sub-lesional spinal segments. We found a near complete, lamina-specific restoration of neurofilament density in denervated segments of chronically injured rats ($P < 0.01$; Fig. 6B and C).

This result suggested that the SCI led to the formation of new arbors in sub-lesional segments, which we evaluated in more detail with neuronal tract-tracing techniques. We injected a TMR-conjugated antero- and retrograde neuronal tracer into spinal segments L1-L2 (Fig. 6A). We first quantified retrogradely labelled neurons at L6 and found a 2-fold increase in the number of labelled neurons in rats with chronic SCI compared with both intact and subacutely lesioned animals ($P < 0.001$; Fig. 6D). We next evaluated the density of anterogradely labelled fibres projecting to L6. The number of labelled fibres at L6 was significantly reduced in the subacute stage ($P < 0.001$), presumably

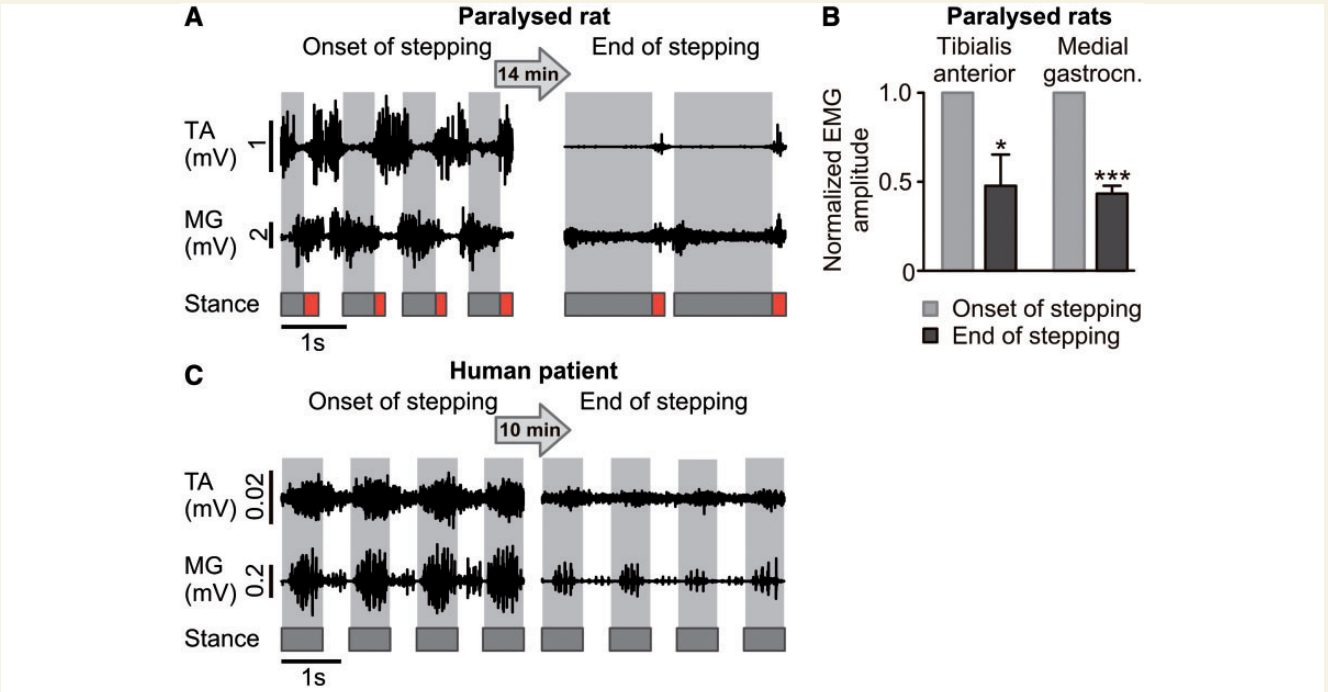

Figure 4 Exhaustion of locomotor muscle activity in the chronic stage of SCI. (**A**) Evaluation of exhaustion of locomotor muscle activity in rats at the chronic stage of SCI. Rats were positioned bipedally over a moving treadmill belt with 90% body weight support at a speed of 9 cm/s. Stepping was enabled with the electrical neuroprosthesis and a representative example of muscle activity is shown at the onset and end of a 14-min continuous stepping bout. (**B**) Bar graphs of the normalized EMG amplitudes recorded at the beginning and end of stepping in rats ($n = 4$). (**C**) Representative example of EMG activity recorded in a chronically paralysed human patient during robotically assisted leg movements at a constant speed of 2.0 km/h and 65–75% body weight support. EMG activity is shown at the onset of stepping and after 10 min of a continuous bout of locomotion. Adapted from Dietz *et al.* (2009). $*P < 0.05$; $***P < 0.001$. Error bars, SEM. MG = medial gastrocnemius; TA = tibialis anterior.

due to the loss of descending fibres. We observed a 3-fold increase in the density of fibres at L6 in the chronic stage of SCI ($P < 0.001$; Fig. 6D and E). This increase in fibre density re-established the level of innervation observed in intact rats ($P = 0.96$; Fig. 6D, right).

To confirm and expand these findings, we next evaluated changes in the density of synapses associated with intraspinal afferent fibres. Glutamate is the most abundant excitatory neurotransmitter in the spinal cord. The vesicular glutamate transporter 2 (vGlut2) is expressed in the synaptic terminals of various spinally projecting supraspinal neurons and intraspinal neurons. Due to the complete interruption of descending pathways after staggered hemisections, vGlut2 is near-exclusively associated with segmental afferents in injured rats (Oliveira *et al.*, 2003; Todd *et al.*, 2003; Alvarez *et al.*, 2004; Landry *et al.*, 2004). vGlut2-positive fibre endings were primarily found in the superficial dorsal horn and in the intermediate and ventral laminae 7 to 10 (Fig. 7B). Compared with intact rats, we found a significant decrease in vGlut2 density in spinal segment L4 of rats in the subacute stage of the SCI ($P < 0.001$; Fig. 7A). Rats in the chronic stage of SCI exhibited a near complete, lamina-specific restoration of vGlut2 density ($P < 0.01$; Fig. 7A and B). These combined results reveal that a striking, lamina-specific reorganization of intraspinal connectivity and associated synaptic terminals spontaneously takes place in the chronic stage of severe SCI.

Staggered hemisection injury leads to remodelling of sensory terminals within denervated segments

We sought to investigate whether sensory afferents also undergo remodelling in response to severe SCI. Staining of vesicular glutamate transporter 1 (vGlut1) in the spinal cord mainly identifies the synaptic terminals of corticospinal fibres (Persson *et al.*, 2006), as well as myelinated primary afferents (Oliveira *et al.*, 2003; Todd *et al.*, 2003; Alvarez *et al.*, 2004; Landry *et al.*, 2004), which essentially arise from muscle proprioceptive fibres (Alvarez *et al.*, 2004). Due to the complete interruption of the corticospinal tract after staggered hemisections, vGlut1 staining provides the opportunity to quantify the density of synaptic contacts formed by proprioceptive fibres in denervated spinal segments. vGlut1-positive fibre endings were concentrated in the deep dorsal horn and around the central canal (Fig. 7D), which complemented the distribution pattern of vGlut2-positive synapses. Compared with intact rats, vGlut1 density was significantly reduced in intermediate and ventral laminae in the subacute stage of the SCI ($P < 0.01$; Fig. 7C). Rats in the chronic stage of SCI showed a density of myelinated primary afferent terminals that did not differ from that observed in intact rats (Fig. 7C). The recovery of vGlut1-positive fibre endings occurred in a lamina-specific manner (Fig. 7D).

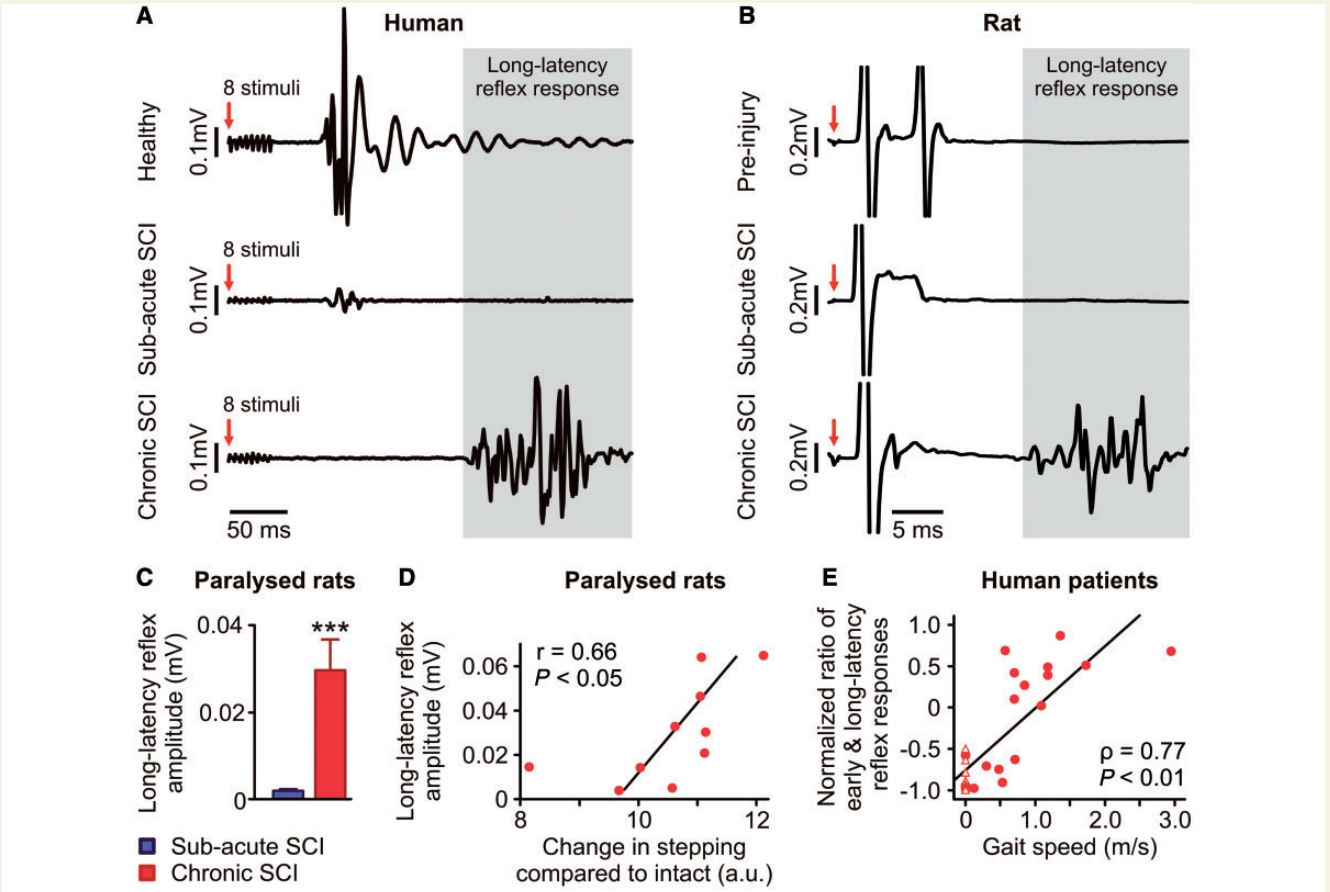

Figure 5 Emergence of long-latency reflex responses in the chronic stage of SCI correlated with deterioration of locomotor capacities. (**A**) Representative reflex traces recorded from the tibialis anterior muscle in response to a train of tibial nerve stimulations in a healthy subject, and a severely paralysed non-ambulatory patient recorded in both the subacute and chronic stage of SCI. Adapted from Dietz *et al.* (2009). (**B**) Representative reflex traces recorded from the tibialis anterior muscle in response to a single epidural stimulus at S1 in the same rat pre-lesion, and in the subacute and chronic stage of SCI. The shaded area highlights the window for the long-latency reflex responses. (**C**) Bar graph reporting the amplitude of the long-latency reflex response in the subacute and chronic stage of SCI in rats ($n = 8$). (**D**) Correlation between stepping capacities and the amplitude of the long-latency reflex response in chronically paralysed rats ($n = 10$). Stepping capacities were quantified as the 3D distance (see Fig. 2) between gait cycles pre-lesion and in the chronic stage of SCI. (**E**) Correlation between the normalized ratio of early and long-latency reflex responses and the walking speed converted from the 10 min walk test in patients with clinically complete (triangle) and incomplete (circle) SCI. Adapted from Hubli *et al.* (2012). $***P < 0.001$. Error bars, SEM. ρ = Spearman's rank correlation coefficient.

Rats with chronic injury show aberrant recruitment of neurons during stepping

We sought to evaluate whether the increased density of fibres and synapses observed in rats with chronic SCI had an impact on the recruitment of sensorimotor circuits during gait execution. To address this question, we studied the expression pattern of the activity-dependent early gene protein c-fos in response to a continuous bout of electrochemically-enabled stepping (Ichiyama *et al.*, 2008; Courtine *et al.*, 2009). Rats in the chronic stage of SCI exhibited a 2-fold increase in the number of c-fos^{on} neurons in motor-related spinal regions (laminae 7 to 10) compared with intact rats ($P < 0.001$; Fig. 8A–C). The number of c-fos^{on} neurons inversely correlated with locomotor capacities ($r = -0.86$, $P < 0.001$; Fig. 8B).

Syndromic analysis establishes relationships between functional and neuromorphological changes after severe injury

We finally aimed at establishing multidirectional correlative relationships between functional, electrophysiological and neuromorphological alterations in chronically injured rats. For this purpose, we applied a syndromic analysis (Ferguson *et al.*, 2013) to all the computed variables ($n = 55$) in order to uncover causal links between neuronal dysfunction and

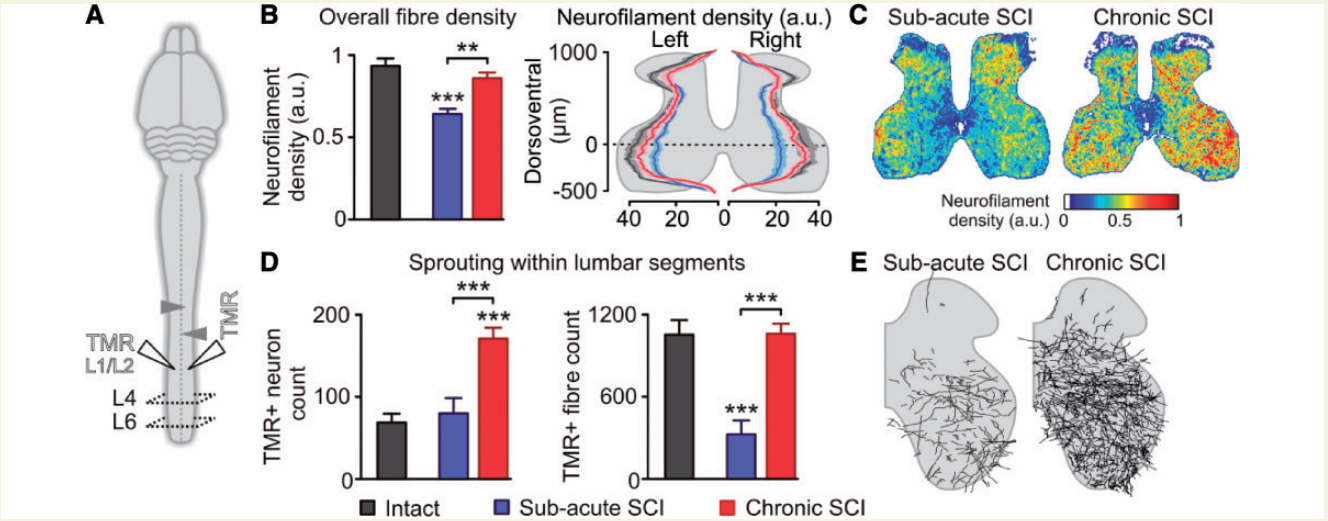

Figure 6 The staggered lateral hemisection SCI led to substantial intraspinal reorganization in the denervated lumbosacral segments. (**A**) Diagram illustrating anatomical experiments. (**B**) Bar graph and density plot reporting the overall neurofilament density and lamina-specific neurofilament density within the spinal segment L4 for each experimental group ($n = 4–5$ rats per group). (**C**) Representative heatmaps displaying neurofilament density throughout the spinal cord grey matter. (**D**) Bar graphs reporting the number of retrogradely labelled neurons at L6, and manual fibre counts at L6 after injecting TMR at L1–L2 ($n = 5–6$ rats per group). (**E**) Single-slice fibre reconstructions of TMR-labelled fibre density in the right L6 hemicord. $^{**}P < 0.01$; $^{***}P < 0.001$. Error bars, SEM.

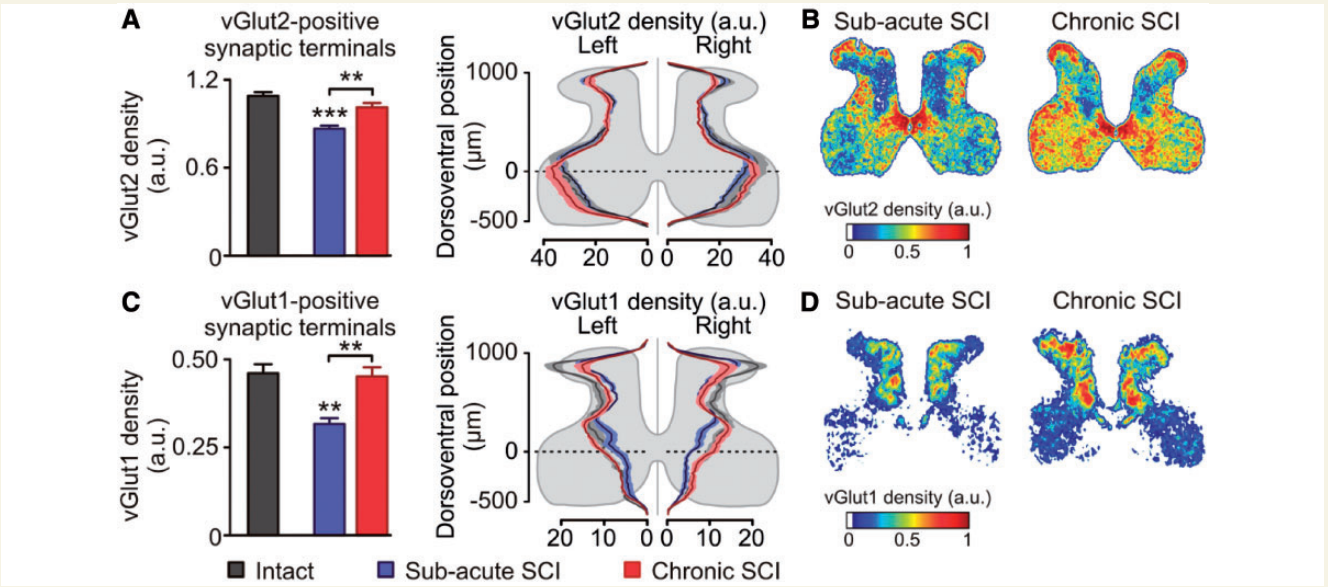

Figure 7 The staggered lateral hemisection SCI led to reorganization of sensory afferents in denervated lumbosacral segments. (**A**) Bar graph and density plot reporting density of vGlut2-positive synaptic terminals in spinal segment L4 ($n = 4–5$ rats per group). (**B**) Representative heatmaps of vGlut2-positive synaptic terminals. (**C**) Bar graph and density plot reporting density of vGlut1-positive synaptic terminals in spinal segment L4 ($n = 4–5$ rats per group). (**D**) Representative heatmaps of vGlut1-positive synaptic terminals. $^{**}P < 0.01$; $^{***}P < 0.001$. Error bars, SEM.

compensatory plasticity. The first principal component analysis accounted for 32% of the total variance (Fig. 9). Extraction of PC1 factor loadings revealed that deterioration of stepping capacities, emergence of long-latency reflex responses, and extensor over-activity during electrochemically enabled motor states significantly correlated with injury-induced reorganization of primary afferent and intraspinal axonal systems. This syndromic analysis thus suggested that the aberrant remodelling of lumbosacral circuits significantly contributed to the syndrome of neuronal dysfunction after a severe SCI.

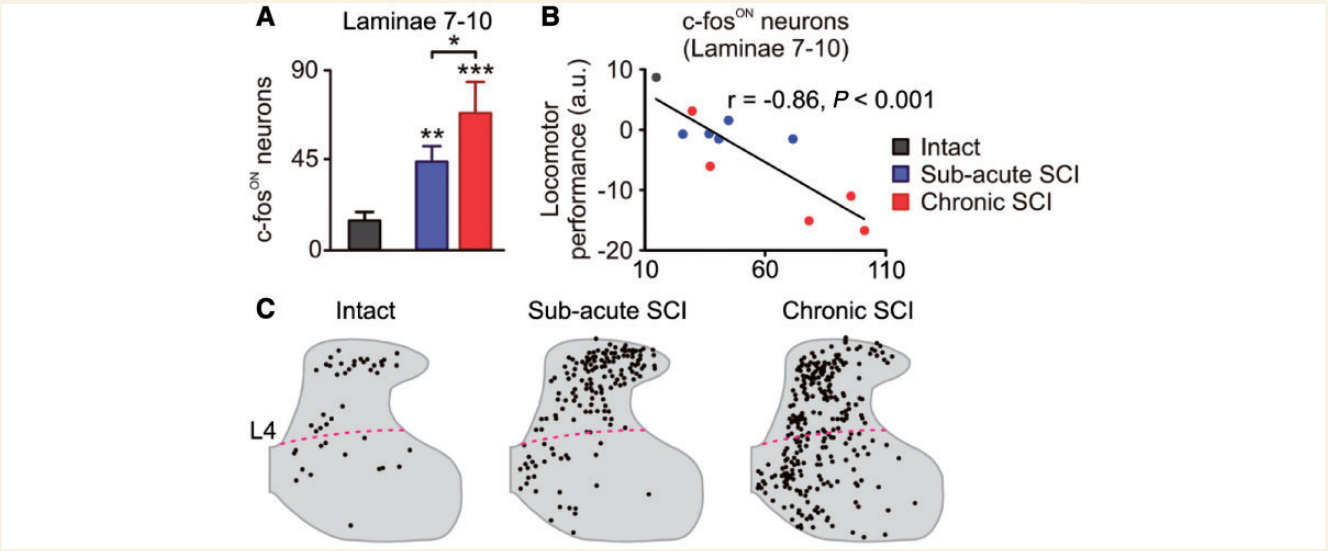

Figure 8 Locomotor activity engaged an aberrant neuronal population in the chronic stage of severe SCI. (**A**) Bar graph reporting the number of c-fos^{ON} neurons in laminae 7–10 of spinal segment after 45 min of continuous stepping ($n = 5$ rats per group). (**B**) Correlation between c-fos^{ON} neuron counts and stepping performance quantified as the sum of PC1 and PC2 for each animal. (**C**) Single-slice reconstructions of c-fos^{ON} neurons in spinal segment L4. Laminae 7–10 are delineated by the dotted line. $*P < 0.05$; $**P < 0.01$; $***P < 0.001$. Error bars, SEM.

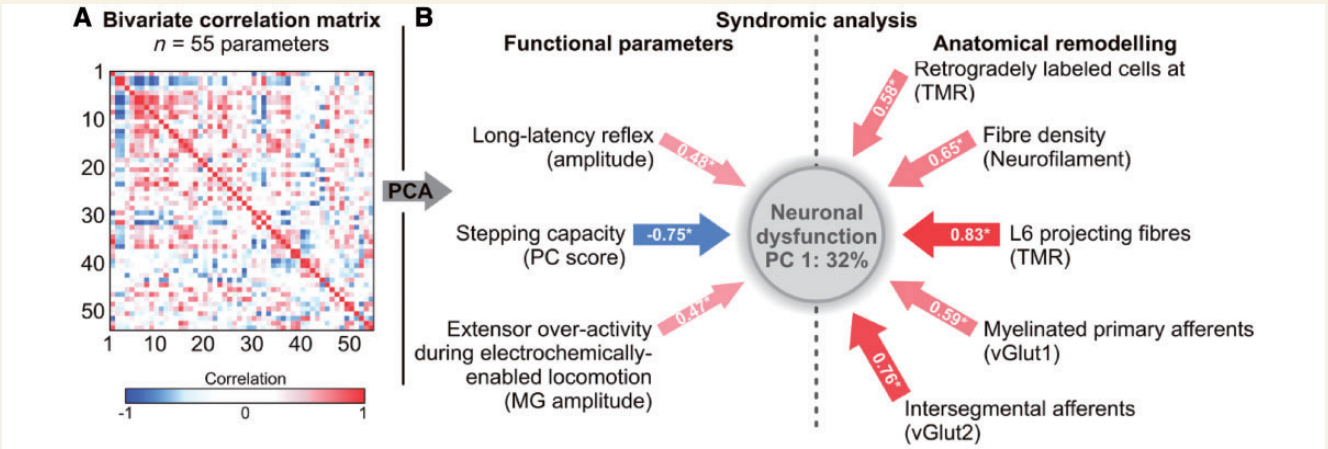

Figure 9 Syndromic analysis establishes relationships between functional and neuromorphological changes after severe SCI. (**A**) Bivariate correlations were applied to all the functional, electrophysiological and neuromorphological variables ($n = 55$) for all the rats in the subacute and chronic stage of the SCI. (**B**) Principal component analysis (PC) was performed on the bivariate correlation matrix and stepping capacities significantly correlated with PC1 (32% of explained variance), indicating that PC1 was associated with the development of neuronal dysfunction. Each arrow represents a functional or neuromorphological variable with a high factor loading on PC1. The thickness of each arrow is proportional to the contribution of each represented variable to PC1. Blue and red colours correspond to a decrease or increase in the values of the variables, respectively. For example, this analysis shows that a decrease in stepping capacities (blue) correlates with an increase in the number of L6 projecting fibres (red). Asterisks indicate statistically significant factor loadings (|value| > 0.45). MG = medial gastrocnemius.

Discussion

We show that chronically paralysed rats and humans exhibited similar changes in locomotor activity and reflex behaviour. Using a syndromic analysis (Ferguson *et al.*, 2013) applied on a range of functional, electrophysiological and neuromorphological assessments, we provide statistical evidence that aberrant remodelling of denervated spinal circuits was in part responsible for the development of neuronal dysfunction in the chronic stage of SCI.

Severely paralysed rats and humans exhibit similar neuronal dysfunction in the chronic stage of injury

We aimed at developing a SCI model that shares some of the key pathophysiological and functional features of a severe SCI in humans. Specifically, we sought to create a lesion that induces permanent paralysis, but spares residual bridges of intact neural tissue (Courtine *et al.*, 2008; Murray *et al.*, 2010). We placed a staggered lateral hemisection SCI that met these criteria while providing controlled experimental conditions to assess injury- and intervention-mediated anatomical reorganization (van den Brand *et al.*, 2012). This SCI induced a neuronal dysfunction in the chronic stage of the injury, which contrasted with the progressive recovery of sensorimotor functions that spontaneously occur after partial spinal cord injuries in rodents (Raineteau and Schwab, 2001; Bareyre *et al.*, 2004; Courtine *et al.*, 2008), non-human primates (Courtine *et al.*, 2005; Rosenzweig *et al.*, 2010) and humans (Curt *et al.*, 2008). Neuronal dysfunction in rats was characterized by a premature exhaustion of locomotor muscle activity, which was also observed in chronic, non-ambulatory patients (Dietz and Muller, 2004); and by a dramatic dysfunction of spinal locomotor circuits that we uncovered with the use of an electrochemical neuroprosthesis (Courtine *et al.*, 2009; Musienko *et al.*, 2012). Although the progressive decline of functional capacities has been well documented after a severe SCI (de Leon *et al.*, 1999; Dietz *et al.*, 2002; Boulenguez *et al.*, 2010) our detailed neurobiomechanical and statistical analyses identified, for the first time, the syndromic signature of deterioration of stepping function in rats. This syndrome included high gait variability, pronounced flexed posture, undesired co-activation between antagonistic muscles, poor interlimb coordination, altered distal joint control, and increased extensor muscle activity during electrochemically enabled locomotion. Comparable changes in gait pattern characteristics have been reported in humans with SCI (Grasso *et al.*, 2004; Lunenburger *et al.*, 2006; McKay *et al.*, 2011). Here, we hypothesized that the development of neuronal dysfunction is largely due to multifaceted plastic changes that propagate throughout local and long-distance interneuronal circuits after severe SCI.

Severely paralysed rats and humans exhibit similar changes in reflex behaviour in the chronic stage of injury

We previously documented the emergence of abnormal long-latency reflex responses in ankle flexor muscles following stimulation of the tibial nerve in non-ambulatory individuals with chronic SCI (Dietz *et al.*, 2009). The amplitude of these reflex responses correlated with the development of neuronal dysfunction (Hubli *et al.*, 2012). These long-latency reflex responses resemble an exacerbation of the flexor reflex afferent response, which plays an important role in the production of locomotion (Bussel *et al.*, 1989; Nicol *et al.*, 1995). To date, this syndrome has never been observed in experimental animals with SCI (Dietz *et al.*, 2009). Here, we developed a new model of SCI in which we observed the appearance of abnormal long-latency reflex responses in the chronic stage of the injury. As previously observed in humans (Hubli *et al.*, 2012), the amplitude of long-latency reflexes correlated with the development of neuronal dysfunction in rats with SCI.

These results highlight remarkable similarities in the functional response of the rodent and human spinal cord after the chronic interruption of supraspinal input. The profound reorganization of sub-lesional reflex circuits suggested that a significant anatomical remodelling took place within denervated neuronal networks after severe SCI.

Undirected plasticity of denervated circuits leads to the development of neuronal dysfunction in the chronic stage of injury

Previous investigations in animal models of SCI documented the progressive upregulation of receptor, synapse and fibre density in spinal circuitries deprived of supraspinal input (Krenz and Weaver, 1998; Kitzman, 2006; Boulenguez *et al.*, 2010; Ichiyama *et al.*, 2011; Kapitza *et al.*, 2012; Tan *et al.*, 2012; Bos *et al.*, 2013). In the present study, we also found a multiplicity of plastic changes in spinal segments caudal to a staggered lateral hemisection SCI. Chronically denervated lumbosacral segments showed sprouting of myelinated primary afferent fibres, increased intraspinal axon density, enhanced bidirectional connectivity between distant spinal segments, and upregulation of the number of glutamatergic synaptic terminals. Using a syndromic analysis (Ferguson *et al.*, 2011, 2013), we established mechanistic relationships between this extensive anatomical reorganization, and the alteration of reflex behaviour and stepping capacities. These results suggested that injury-induced rewiring of denervated spinal segments formed aberrant sensorimotor circuits that caused abnormal reflex responses and recruited inappropriate combinations of neuronal networks during gait execution. Complementary experimental results directly supported this conclusion; analysis of stepping-associated c-fos expression patterns revealed that rats with chronic SCI engaged an abnormally high number of spinal neurons to produce locomotor output.

These combined results reveal that the interruption of supraspinal pathways induces a profound rewiring within denervated spinal segments, which can lead to the formation of aberrant sensorimotor circuits in the chronic stage of the injury. We suggest that these newly established connections misdirect neural information in spinal circuits during gait execution, which leads to the syndrome of neuronal dysfunction in paralysed rats, and probably in non-ambulatory humans with SCI.

Undirected compensatory plasticity is responsible for the detrimental rewiring of lumbosacral circuits after severe injury

Our results provide overwhelming evidence that a massive reorganization of neural connectivity occurred in denervated spinal

segments after severe SCI. At first these extensive and ubiquitous changes seemed to be chaotic. However, a closer examination suggested that they follow a common biological principle. Injury-induced anatomical reorganization of denervated neural systems occurred in a lamina-specific manner. Changes in the density of fibres and synapses in each lamina at the chronic stage of the SCI invariably reached the innervation level observed in non-injured rats. These results highlight the systematic effort of denervated neural systems to restore their normal synaptic environment. Along the same line, blockage of synaptic transmission induces a substantial increase in the number of dendritic spines on hippocampal neurons (Kirov and Harris, 1999). This phenomenon, which has been termed homeostatic plasticity (Turrigiano *et al.*, 1998), is interpreted as an attempt to maintain a well-balanced synaptic activity in neuronal networks. After incomplete SCIs that leave residual motor capacities, activity-dependent mechanisms likely contribute to steering plasticity. The associated reconfiguration of the synaptic environment promotes useful remodelling that ameliorates sensorimotor functions (Raineteau and Schwab, 2001; Weidner *et al.*, 2001; Edgerton *et al.*, 2004; Courtine *et al.*, 2008; Rosenzweig *et al.*, 2010). For instance, lamina-specific restoration of serotonergic projections in segments caudal to a moderate SCI has been associated with improved locomotion in rats (Mullner *et al.*, 2008).

In contrast, we show here that after a severe SCI leading to chronic paralysis, the absence of activity leads to a chaotic remodelling of denervated neuronal networks. The resulting undirected compensatory plasticity leads to neuronal dysfunction in the chronic stage of SCI. This potentially detrimental impact of compensatory plasticity has been described in other neural networks, including the autonomic nervous system such as the pyloric network of the stomatogastric ganglion (Nahar *et al.*, 2012). In the spinal cord, the increased expression of constitutively active 5-HT_{2C} receptor isoforms partially compensated for the depletion of brainstem-derived serotonin after severe SCI (Murray *et al.*, 2010). However, the regained excitability in motor neurons contributed to the development of abnormal reflex responses (Murray *et al.*, 2010). Likewise, the depletion of corticospinal tract associated vGlut1 terminals after a pyramidotomy induced a specific sprouting of vGlut1 proprioceptive afferent fibres, but also in this condition, the synaptic reorganization adversely altered proprioceptive reflex circuits (Tan *et al.*, 2012). Although additional mechanisms such as changes in motor neuron membrane excitability (Lin *et al.*, 2007; Boulenguez *et al.*, 2010) likely contribute to neuronal dysfunction in the chronic stage of SCI, our combined results suggest that undirected compensatory plasticity plays an important role in the emergence of this syndrome.

Directing compensatory plasticity to improve functional recovery after severe injury

We propose that the myriad of anatomical and functional changes that follow a severe SCI obeys a common biological principle—compensatory plasticity, which is a powerful mechanism to maintain the stability of neurons, and shape the reconfiguration of circuits and pathways following injury (Turrigiano *et al.*, 1998). However, unless this process is directed with use-dependent cues, compensatory plasticity can lead to an aberrant reorganization of denervated spinal circuits, which contributes to the development of neuronal dysfunction in the chronic stage of SCI.

Spinal cord repair interventions primarily focus on developing strategies to promote regeneration of severed neural pathways. The present findings in rats and humans demonstrate that recovery after severe SCI will also necessitate directing and exploiting compensatory plasticity to preserve and improve the functional capacities of denervated spinal sensorimotor circuits (Dietz, 2010). Electrochemically-enabled training is capable of promoting useful remodelling of spinal circuits and functional improvement in severely paralysed rats (Ichiyama *et al.*, 2008, 2011; Courtine *et al.*, 2009; van den Brand *et al.*, 2012). Robotically assisted training also shows efficacy to improve both spinal reflex behaviour and mobility in individuals with incomplete SCI (Hubli *et al.*, 2012). Future studies will need to investigate how activity-based rehabilitation steers compensatory plasticity of spinal sensorimotor circuits in order to prevent, and potentially reverse, the development of neuronal dysfunction after severe SCI.

Acknowledgements

We thank Nadja Kaufmann, Mathias Roth, Kay Bartholdi, Michèle Huerlimann and Simone Duis for help and support with surgeries, animal care and data collection.

Funding

This work was supported by the National Center of Competence in Research (NCCR) "Plasticity and Repair" of the Swiss National Science Foundation; a Starting Grant from the European Research Council [ERC 261247, *Walk Again*]; the Neuroscience Centre Zurich (ZNZ); the European Community's Seventh Framework Program [CP-IP 258654, *NEUWalk*]; and funding from the Swiss National Science Foundation [subside 310030_130850].

References

Alvarez FJ, Villalba RM, Zerda R, Schneider SP. Vesicular glutamate transporters in the spinal cord, with special reference to sensory primary afferent synapses. J Comp Neurol 2004; 472: 257–80.

Ballermann M, Fouad K. Spontaneous locomotor recovery in spinal cord injured rats is accompanied by anatomical plasticity of reticulospinal fibers. Eur J Neurosci 2006; 23: 1988–96.

Bareyre FM, Kerschensteiner M, Raineteau O, Mettenleiter TC, Weinmann O, Schwab ME. The injured spinal cord spontaneously forms a new intraspinal circuit in adult rats. Nat Neurosci 2004; 7: 269–77.

Beres-Jones JA, Johnson TD, Harkema SJ. Clonus after human spinal cord injury cannot be attributed solely to recurrent muscle-tendon stretch. Exp Brain Res 2003; 149: 222–36.

Bos R, Sadlaoud K, Boulenguez P, Buttigieg D, Liabeuf S, Brocard C, et al. Activation of 5-HT2A receptors upregulates the function of the neuronal K-Cl cotransporter KCC2. Proc Natl Acad Sci USA 2013; 110: 348–53.

Boulenguez P, Liabeuf S, Bos R, Bras H, Jean-Xavier C, Brocard C, et al. Down-regulation of the potassium-chloride cotransporter KCC2 contributes to spasticity after spinal cord injury. Nat Med 2010; 16: 302–7.

Bussel B, Roby-Brami A, Yakovleff A, Bennis N. Late flexion reflex in paraplegic patients. Evidence for a spinal stepping generator. Brain Res Bull 1989; 22: 53–6.

Calancie B, Alexeeva N, Broton JG, Molano MR. Interlimb reflex activity after spinal cord injury in man: strengthening response patterns are consistent with ongoing synaptic plasticity. Clin Neurophysiol 2005; 116: 75–86.

Calancie B, Lutton S, Broton JG. Central nervous system plasticity after spinal cord injury in man: interlimb reflexes and the influence of cutaneous stimulation. Electroencephalogr Clin Neurophysiol 1996; 101: 304–15.

Calancie B, Molano MR, Broton JG. Neural plasticity as revealed by the natural progression of movement expression-both voluntary and involuntary—in humans after spinal cord injury. Prog Brain Res 2000; 128: 71–88.

Carmel JB, Berrol LJ, Brus-Ramer M, Martin JH. Chronic electrical stimulation of the intact corticospinal system after unilateral injury restores skilled locomotor control and promotes spinal axon outgrowth. J Neurosci 2010; 30: 10918–26.

Courtine G, Gerasimenko Y, van den Brand R, Yew A, Musienko P, Zhong H, et al. Transformation of nonfunctional spinal circuits into functional states after the loss of brain input. Nat Neurosci 2009; 12: 1333–42.

Courtine G, Roy RR, Raven J, Hodgson J, McKay H, Yang H, et al. Performance of locomotion and foot grasping following a unilateral thoracic corticospinal tract lesion in monkeys (Macaca mulatta). Brain 2005; 128 (Pt 10): 2338–58.

Courtine G, Song B, Roy RR, Zhong H, Herrmann JE, Ao Y, et al. Recovery of supraspinal control of stepping via indirect propriospinal relay connections after spinal cord injury. Nat Med 2008; 14: 69–74.

Curt A, van Hedel HJ, Klaus D, Dietz V. Recovery from a spinal cord injury: significance of compensation, neural plasticity, and repair. J Neurotrauma 2008; 25: 677–85.

de Leon RD, Hodgson JA, Roy RR, Edgerton VR. Retention of hindlimb stepping ability in adult spinal cats after the cessation of step training. J Neurophysiol 1999; 81: 85–94.

Dietz V. Behavior of spinal neurons deprived of supraspinal input. Nat Rev Neurol 2010; 6: 167–74.

Dietz V, Grillner S, Trepp A, Hubli M, Bolliger M. Changes in spinal reflex and locomotor activity after a complete spinal cord injury: a common mechanism? Brain 2009; 132 (Pt 8): 2196–205.

Dietz V, Muller R. Degradation of neuronal function following a spinal cord injury: mechanisms and countermeasures. Brain 2004; 127 (Pt 10): 2221–31.

Dietz V, Muller R, Colombo G. Locomotor activity in spinal man: significance of afferent input from joint and load receptors. Brain 2002; 125 (Pt 12): 2626–34.

Dominici N, Keller U, Vallery H, Friedli L, van den Brand R, Starkey ML, et al. Versatile robotic interface to evaluate, enable and train locomotion and balance after neuromotor disorders. Nat Med 2012; 18: 1142–7.

Edgerton VR, Tillakaratne NJ, Bigbee AJ, de Leon RD, Roy RR. Plasticity of the spinal neural circuitry after injury. Annu Rev Neurosci 2004; 27: 145–67.

Fawcett JW, Curt A, Steeves JD, Coleman WP, Tuszynski MH, Lammertse D, et al. Guidelines for the conduct of clinical trials for spinal cord injury as developed by the ICCP panel: spontaneous recovery after spinal cord injury and statistical power needed for therapeutic clinical trials. Spinal Cord 2007; 45: 190–205.

Ferguson AR, Irvine KA, Gensel JC, Nielson JL, Lin A, Ly J, et al. Derivation of multivariate syndromic outcome metrics for consistent testing across multiple models of cervical spinal cord injury in rats. PLoS One 2013; 8: e59712.

Ferguson AR, Stuck ED, Nielson JL. Syndromics: a bioinformatics approach for neurotrauma research. Transl Stroke Res 2011; 2: 438–54.

Gerasimenko YP, Lavrov IA, Courtine G, Ichiyama RM, Dy CJ, Zhong H, et al. Spinal cord reflexes induced by epidural spinal cord stimulation in normal awake rats. J Neurosci Methods 2006; 157: 253–63.

Grasso R, Ivanenko YP, Zago M, Molinari M, Scivoletto G, Castellano V, et al. Distributed plasticity of locomotor pattern generators in spinal cord injured patients. Brain 2004; 127 (Pt 5): 1019–34.

Harkema SJ. Plasticity of interneuronal networks of the functionally isolated human spinal cord. Brain Res Rev 2008; 57: 255–64.

Hausmann ON. Post-traumatic inflammation following spinal cord injury. Spinal Cord 2003; 41: 369–78.

Hiersemenzel LP, Curt A, Dietz V. From spinal shock to spasticity: neuronal adaptations to a spinal cord injury. Neurology 2000; 54: 1574–82.

Horst M, Heutschi J, den Brand R, Andersson KE, Gobet R, Sulser T, et al. Multi-system neuroprosthetic training improves bladder function after severe spinal cord injury. J Urol 2012; 189: 747–53.

Hou S, Duale H, Cameron AA, Abshire SM, Lyttle TS, Rabchevsky AG. Plasticity of lumbosacral propriospinal neurons is associated with the development of autonomic dysreflexia after thoracic spinal cord transection. J Comp Neurol 2008; 509: 382–99.

Hou S, Duale H, Rabchevsky AG. Intraspinal sprouting of unmyelinated pelvic afferents after complete spinal cord injury is correlated with autonomic dysreflexia induced by visceral pain. Neuroscience 2009; 159: 369–79.

Hubli M, Dietz V, Bolliger M. Spinal reflex activity: a marker for neuronal functionality after spinal cord injury. Neurorehabil Neural Repair 2012; 26: 188–96.

Ichiyama RM, Broman J, Roy RR, Zhong H, Edgerton VR, Havton LA. Locomotor training maintains normal inhibitory influence on both alpha- and gamma-motoneurons after neonatal spinal cord transection. J Neurosci 2011; 31: 26–33.

Ichiyama RM, Courtine G, Gerasimenko YP, Yang GJ, van den Brand R, Lavrov IA, et al. Step training reinforces specific spinal locomotor circuitry in adult spinal rats. J Neurosci 2008; 28: 7370–5.

Kapitza S, Zorner B, Weinmann O, Bolliger M, Filli L, Dietz V, et al. Tail spasms in rat spinal cord injury: changes in interneuronal connectivity. Exp Neurol 2012; 236: 179–89.

Kirov SA, Harris KM. Dendrites are more spiny on mature hippocampal neurons when synapses are inactivated. Nat Neurosci 1999; 2: 878–83.

Kitzman P. Changes in vesicular glutamate transporter 2, vesicular GABA transporter and vesicular acetylcholine transporter labeling of sacrocaudal motoneurons in the spastic rat. Exp Neurol 2006; 197: 407–19.

Kitzman P. VGLUT1 and GLYT2 labeling of sacrocaudal motoneurons in the spinal cord injured spastic rat. Exp Neurol 2007; 204: 195–204.

Krenz NR, Weaver LC. Sprouting of primary afferent fibers after spinal cord transection in the rat. Neuroscience 1998; 85: 443–58.

Landry M, Bouali-Benazzouz R, El Mestikawy S, Ravassard P, Nagy F. Expression of vesicular glutamate transporters in rat lumbar spinal cord, with a note on dorsal root ganglia. J Comp Neurol 2004; 468: 380–94.

Lavrov I, Gerasimenko YP, Ichiyama RM, Courtine G, Zhong H, Roy RR, et al. Plasticity of spinal cord reflexes after a complete transection in adult rats: relationship to stepping ability. J Neurophysiol 2006; 96: 1699–710.

Lin CS, Macefield VG, Elam M, Wallin BG, Engel S, Kiernan MC. Axonal changes in spinal cord injured patients distal to the site of injury. Brain 2007; 130 (Pt 4): 985–94.

Lunenburger L, Bolliger M, Czell D, Muller R, Dietz V. Modulation of locomotor activity in complete spinal cord injury. Exp Brain Res 2006; 174: 638–46.

Maegele M, Muller S, Wernig A, Edgerton VR, Harkema SJ. Recruitment of spinal motor pools during voluntary movements versus stepping after human spinal cord injury. J Neurotrauma 2002; 19: 1217–29.

McKay WB, Ovechkin AV, Vitaz TW, Terson de Paleville DG, Harkema SJ. Long-lasting involuntary motor activity after spinal cord injury. Spinal Cord 2011; 49: 87–93.

Molander C, Xu Q, Grant G. The cytoarchitectonic organization of the spinal cord in the rat. I. The lower thoracic and lumbosacral cord. J Comp Neurol 1984; 230: 133–41.

Mullner A, Gonzenbach RR, Weinmann O, Schnell L, Liebscher T, Schwab ME. Lamina-specific restoration of serotonergic projections after Nogo-A antibody treatment of spinal cord injury in rats. Eur J Neurosci 2008; 27: 326–33.

Murray KC, Nakae A, Stephens MJ, Rank M, D'Amico J, Harvey PJ, et al. Recovery of motoneuron and locomotor function after spinal cord injury depends on constitutive activity in 5-HT2C receptors. Nat Med 2010; 16: 694–700.

Musienko P, Heutschi J, Friedli L, van den Brand R, Courtine G. Multi-system neurorehabilitative strategies to restore motor functions following severe spinal cord injury. Exp Neurol 2012; 235: 100–9.

Musienko P, van den Brand R, Marzendorfer O, Roy RR, Gerasimenko Y, Edgerton VR, et al. Controlling specific locomotor behaviors through multidimensional monoaminergic modulation of spinal circuitries. J Neurosci 2011; 31: 9264–78.

Nahar J, Lett KM, Schulz DJ. Restoration of descending inputs fails to rescue activity following deafferentation of a motor network. J Neurophysiol 2012; 108: 871–81.

Nicol DJ, Granat MH, Baxendale RH, Tuson SJ. Evidence for a human spinal stepping generator. Brain Res 1995; 684: 230–2.

Oliveira AL, Hydling F, Olsson E, Shi T, Edwards RH, Fujiyama F, et al. Cellular localization of three vesicular glutamate transporter mRNAs and proteins in rat spinal cord and dorsal root ganglia. Synapse 2003; 50: 117–29.

Persson S, Boulland JL, Aspling M, Larsson M, Fremeau RT Jr, Edwards RH, et al. Distribution of vesicular glutamate transporters 1 and 2 in the rat spinal cord, with a note on the spinocervical tract. J Comp Neurol 2006; 497: 683–701.

Raineteau O, Schwab ME. Plasticity of motor systems after incomplete spinal cord injury. Nat Rev Neurosci 2001; 2: 263–73.

Riegger T, Conrad S, Schluesener HJ, Kaps HP, Badke A, Baron C, et al. Immune depression syndrome following human spinal cord injury (SCI): a pilot study. Neuroscience 2009; 158: 1194–9.

Rosenzweig ES, Courtine G, Jindrich DL, Brock JH, Ferguson AR, Strand SC, et al. Extensive spontaneous plasticity of corticospinal projections after primate spinal cord injury. Nat Neurosci 2010; 13: 1505–10.

Roy RR, Edgerton VR. Neurobiological perspective of spasticity as occurs after a spinal cord injury. Exp Neurol 2012; 235: 116–22.

Singh A, Balasubramanian S, Murray M, Lemay M, Houle J. Role of spared pathways in locomotor recovery after body-weight-supported treadmill training in contused rats. J Neurotrauma 2011; 28: 2405–16.

Soares S, Barnat M, Salim C, von Boxberg Y, Ravaille-Veron M, Nothias F. Extensive structural remodeling of the injured spinal cord revealed by phosphorylated MAP1B in sprouting axons and degenerating neurons. Eur J Neurosci 2007; 26: 1446–61.

Tan AM, Chakrabarty S, Kimura H, Martin JH. Selective corticospinal tract injury in the rat induces primary afferent fiber sprouting in the spinal cord and hyperreflexia. J Neurosci 2012; 32: 12896–908.

Tan AM, Stamboulian S, Chang YW, Zhao P, Hains AB, Waxman SG, et al. Neuropathic pain memory is maintained by Rac1-regulated dendritic spine remodeling after spinal cord injury. J Neurosci 2008; 28: 13173–83.

Todd AJ, Hughes DI, Polgar E, Nagy GG, Mackie M, Ottersen OP, et al. The expression of vesicular glutamate transporters VGLUT1 and VGLUT2 in neurochemically defined axonal populations in the rat spinal cord with emphasis on the dorsal horn. Eur J Neurosci 2003; 17: 13–27.

Turrigiano GG, Leslie KR, Desai NS, Rutherford LC, Nelson SB. Activity-dependent scaling of quantal amplitude in neocortical neurons. Nature 1998; 391: 892–6.

Tuszynski MH, Steward O. Concepts and methods for the study of axonal regeneration in the CNS. Neuron 2012; 74: 777–91.

van den Brand R, Heutschi J, Barraud Q, DiGiovanna J, Bartholdi K, Huerlimann M, et al. Restoring voluntary control of locomotion after paralyzing spinal cord injury. Science 2012; 336: 1182–5.

Weidner N, Ner A, Salimi N, Tuszynski MH. Spontaneous corticospinal axonal plasticity and functional recovery after adult central nervous system injury. Proc Natl Acad Sci USA 2001; 98: 3513–8.